Neuro-Oncology Advances
2(1), 1–10, 2020 | doi:10.1093/noajnl/vdaa028 | Advance Access date 28 February 2020

Responses in the diffusivity and vascular function of the irradiated normal brain are seen up until 18 months following SRS of brain metastases

Line Brennhaug Nilsen, Ingrid Digernes, Endre Grøvik, Cathrine Saxhaug, Anna Latysheva, Oliver Geier, Birger Breivik, Dag Ottar Sætre, Kari Dolven Jacobsen, Åslaug Helland, and Kyrre Eeg Emblem

Department of Diagnostic Physics, Oslo University Hospital, Oslo, Norway (L.B.N., I.D., E.G., O.G., K.E.E.); Department of Radiology and Nuclear Medicine, Oslo University Hospital, Oslo, Norway (C.S., A.L.); Department of Radiology, Hospital of Southern Norway, Kristiansand, Norway (B.B.); Department of Radiology, Østfold Hospital Trust, Klanes, Norway (D.O.S.); Department of Oncology, Oslo University Hospital, Oslo, Norway (K.D.J., ÅH); University of Oslo, Oslo, Norway (I.D.)

Corresponding Author: Line Brennhaug Nilsen PhD, Department of Diagnostic Physics, Oslo University Hospital, Building 20 Gaustad, P.O. Box 4959 Nydalen, N-0424 Oslo, Norway (line.nilsen2@rr-research.no).

Abstract

Background. MRI may provide insights into longitudinal responses in the diffusivity and vascular function of the irradiated normal-appearing brain following stereotactic radiosurgery (SRS) of brain metastases.

Methods. Forty patients with brain metastases from non-small cell lung cancer ($N = 26$) and malignant melanoma ($N = 14$) received SRS (15–25 Gy). Longitudinal MRI was performed pre-SRS and at 3, 6, 9, 12, and 18 months post-SRS. Measures of tissue diffusivity and vascularity were assessed by diffusion-weighted and perfusion MRI, respectively. All maps were normalized to white matter receiving less than 1 Gy. Longitudinal responses were assessed in normal-appearing brain, excluding tumor and edema, in the LowDose (1–10 Gy) and HighDose (>10 Gy) regions. The Eastern Cooperative Oncology Group (ECOG) performance status was recorded pre-SRS.

Results. Following SRS, the diffusivity in the LowDose region increased continuously for 1 year (105.1% ± 6.2%; $P < .001$), before reversing toward pre-SRS levels at 18 months. Transient reductions in microvascular cerebral blood volume ($P < .05$), blood flow ($P < .05$), and vessel densities ($P < .05$) were observed in LowDose at 6–9 months post-SRS. Correspondingly, vessel calibers in LowDose transiently increased at 3–9 months ($P < .01$). The responses in HighDose displayed similar trends as in LowDose, but with larger interpatient variations. Vascular responses followed pre-SRS ECOG status.

Conclusions. Our results imply that even low doses of radiation to normal-appearing brain following cerebral SRS induce increased diffusivity and reduced vascular function for up until 18 months. In particular, the vascular responses indicate the reduced ability of the normal-appearing brain tissue to form new capillaries. Assessing the potential long-term neurologic effects of SRS on the normal-appearing brain is warranted.

Key Points

- SRS increased diffusivity and reduced microvascular function in normal-appearing brain tissue.
- Increased diffusivity and reduced microvascular function were observed in low-dose regions.
- Microvascular changes were associated with the pre-SRS ECOG status.

Importance of the Study

Stereotactic radiosurgery (SRS) is a well-established treatment option for cancer patients with a limited number of brain metastases (<5). Although SRS inherently provides rapid dose fall-off to surrounding normal-appearing brain tissue, several preclinical studies suggest that damage to the vascular network plays a key role in radiation-induced effects in a normal brain. However, a complete understanding of underlying radiobiological responses in the surrounding normal brain and the impact on neurologic function are missing. To address this need, we here demonstrate increased diffusivity and reduced vascular function in the normal-appearing brain parenchyma in patients with brain metastases treated with SRS even in low-dose regions until 18 months follow-up. Our results suggest that mapping tissue diffusivity and vascular function prior to treatment may bring us closer to revealing the underlying functional mechanisms of SRS.

Stereotactic radiosurgery (SRS) is a well-established first-line treatment option for patients with a limited number of brain metastases (<5) and good performance status.[1] Compared to the combined use of SRS and whole-brain radiotherapy (WBRT), or WBRT alone, SRS alone provides similar survival rates, but reduced risk of harm to neurocognition and quality of life.[2,3] Due to continuous improvements in image-guided identification of targets and organs at risk, as well as in radiation delivery techniques, SRS is also becoming increasingly attractive in cases of multiple metastases.[1]

Brain radionecrosis is the most common complication after SRS, reported to occur in 24% of patients and causing neurological deficits in 13%.[4] Over the past decades, studies have identified the dosimetric burden on surrounding normal brain to be an important risk factor for the development of radionecrosis, ie, the risk increases if the volume of brain exposed to doses higher than a threshold dose, typically 10–12 Gy, is above 5–10 cc.[4,5] However, a complete understating of the underlying radiobiological response mechanisms governing the development of radiation-induced toxicity and followed radionecrosis is missing. Moreover, the relevance of lower doses from SRS (<8 Gy) to normal-appearing brain for potential long-term effects is poorly understood.[5]

Several preclinical studies have recognized damage to the vascular network to play a key role in radiation-induced effects on normal brain tissue.[6] Radiation-induced vascular damage involves early endothelial cell injury and apoptosis, followed by decreased vessel densities, dilation, and thickening of the blood vessels.[7] Additionally, microvessel thrombosis with vessel occlusion may occur within weeks to years after irradiation. In patients, increased vessel permeability in normal-appearing brain tissue, measured by perfusion MRI during fractionated radiotherapy of low-grade gliomas, has been shown to correlate with reduced neurocognitive function.[8] However, clinical studies of vascular responses in irradiated normal-appearing brain tissue are sparse, and most studies have evaluated acute and early responses to fractionated radiotherapy rather than SRS.

To this end, our study sheds light on responses in the diffusivity and vascular function of irradiated non-cancerous normal-appearing brain tissue following SRS of brain metastases from non-small cell lung cancer and malignant melanomas.

Material and Methods

Patients and Study Design

Forty patients with brain metastases from non-small cell lung cancer (N = 26) and malignant melanoma (N = 14), participating in an ongoing observational MRI study (TREATMENT; clinicaltrials.gov identifier: NCT03458455), have been analyzed. The study has been approved by the Regional Ethical Committee and written informed consent was obtained from all participants. To be eligible for inclusion, patients must receive SRS to at least one untreated brain metastasis with the longest diameter >5 mm on a diagnostic MRI exam, henceforth referred to as the pre-SRS MRI. Patient, tumor, and treatment characteristics are provided in Supplementary Table 1.

Ten patients had previously received WBRT (N = 4), SRS (N = 3), or both (N = 3) to other metastases not targeted by SRS in this study. Furthermore, 5 patients received concomitant immunotherapy. Eighteen patients were using corticosteroids (individual dosage) at the pre-SRS MRI, while 21 patients did not (information from one patient was not attainable).

At the time of study data lock, MRI exams were performed every 3 months for the first year and at 18 months post-SRS. Dropout of patients on follow-up MRIs was due to death (N = 7), deemed clinically unfit to perform an MRI exam (N = 9), or too short follow-up time (N = 3). The first follow-up MRI at 3 months post-SRS was performed within a margin of 1 week, while the remaining MRI exams were performed within a 2-week margin. After SRS, 12 patients were treated with additional WBRT (N = 4) or SRS (N = 7) or both (N = 1). MRI exams performed on these patients after the additional brain radiotherapy were excluded from further analysis, leaving the following number of patients at each MRI readout: N = 40 (pre-SRS), N = 38 (+3 months), N = 29 (+6 months), N = 22 (+9 months), N = 18 (+12 months), and N = 15 (+18 months).

Stereotactic Radiosurgery

SRS was delivered using a frameless linear accelerator-based system (Varian TrueBeam vSTx, HD-MLC 120; multileaf collimator of 2.5 mm). The SRS planning was mainly performed using iPlan RT Dose (v4.5.4, Brainlab AG). RayStation (v5.0, Raysearch Laboratories) was used in one case. Pre-SRS 3D high-resolution T1-weighted post-contrast MRIs (distortion-corrected) were used for delineation of the metastases and organs at risk, while dose calculation was performed on co-registered computer tomography (CT) images. The time from the pre-SRS MRI to the planning CT scan was on average 4 days (range: 5–12 days). Delineation of the gross tumor volume was performed by a radiation oncologist. A 2 mm isotropic margin, accounting for both subclinical disease and planning uncertainties, was automatically added by the software to generate the planning target volume. The SRS dose was set to cover at least 99% of the planning target volume and ranged from 15 to 25 Gy (single fraction) or from 20.1 to 27 Gy (3 fractions) (Supplementary Table 1). The SRS dose and fractionation scheme were determined according to institutional guidelines, which are based on previous treatment history and clinical status of the patient together with tumor size, proximity to organs at risk, and normal tissue dose constraints. The mean volume of study metastases was significantly lower in patients treated with 1 versus 3 fractions (Supplementary Figure 1).

All patients received a corticosteroid dose (Medrol) of 32 mg (single fraction) or 16 mg (3 fractions) immediately after SRS and on the same night, as well as the following day (morning and night). Those treated with 3 fractions continued to receive 2 doses every day until the night of the last fraction. Thereafter, the use of corticosteroids was individually managed by the patients treating physicians.

MRI Protocol

All MRI exams were performed using a dedicated 20-channel head/neck coil on a 3 T Skyra (Siemens Healthineers) with the following protocol: 3D T1-weighted images, before and after injection of Gadolinium-based contrast agent (Dotarem 279.3 mg/mL, 0.2 mL/kg bodyweight; repetition time [TR]/echo time [TE] = 700 ms/12 ms; voxel size = 0.9 × 0.9 × 0.9 mm^3; acquisition matrix = 512 × 512), T2-weighted fluid attenuated inversion recovery (FLAIR) (TR/TE/inversion time [TI] = 5000 ms/387 ms/1800 ms; voxel size = 0.9 × 0.9 × 0.9 mm^3; acquisition matrix = 512 × 512; field of view = 460.8 × 460.8 mm^2), diffusion-weighted imaging (TR/TE = 5960 ms/71 ms; *b*-values = 0 and 1000/1500 s/mm^2; voxel size = 1.22 × 1.22 × 4.0 mm^3; slice gap = 5.0 mm; acquisition matrix = 180 × 180; field of view = 219.6 × 219.6 mm^2), and dynamic susceptibility contrast (DSC) MRI with combined gradient-echo and spin-echo acquisitions (TR = 1500 ms; TE [gradient-echo] = 13 ms [malignant melanoma]/15–30 ms [non-small cell lung cancer]; TE [spin-echo] = 104 ms; voxel size = 2.0–2.2 × 2.0–2.2 × 5.0 mm^3; slice gap = 6.5 mm; acquisition matrix = 120 × 90; field of view = 240–264 × 180–198 mm^2) with a bolus injection (3 mL/s) of contrast agent, followed by 30 mL of physiologic saline solution.

Co-registration of Dose Distribution and Longitudinal MRI Data

The planning CT images and corresponding SRS dose distribution were exported from the planning system and co-registered to the pre-SRS high-resolution T1-weighted post-contrast MRIs using normalized mutual information in SPM12 (Statistical Parametric Mapping [SPM] toolbox version 12, University College London, England). For each MRI exam, diffusion-weighted images, high-resolution post-contrast and FLAIR images, with associated tumor, edema, as well as binary white and gray matter masks, were co-registered to the DSC MRI space by means of normalized mutual information in nordicICE (NordicNeuroLab AS) or SMP12. Additionally, for the pre-SRS MRIs, the dose distribution was co-registered to the DSC MRI space via the T1-weighted post-contrast MRIs. The pre-SRS DSC space was used as the reference space for co-registration of all longitudinal MRI data. Hence, after final co-registration, the data from all follow-up MRIs and SRS dose distribution were in the pre-SRS DSC space.

Normal-Appearing Brain

White and gray matter was identified on high-resolution T1-weighted post-contrast or FLAIR images by calculation of probability density maps using the segmentation tool in SPM12. The binary masks of white and gray matter were obtained by applying a probability threshold of >0.85 (1.0 being the highest probability). Normal-appearing brain tissue was defined by the white and gray matter masks, excluding areas with pathological contrast enhancement and edema. The pathological contrast enhancement, not excluding central necrosis, was delineated on the high-resolution T1-weighted post-contrast images by 2 experienced neuro-radiologists. Edema was defined on FLAIR images in native or DSC MRI space. All delineations were performed in nordicICE.

The co-registered dose distribution (Figure 1A) was divided into 3 distinct isodose levels: Reference <1 Gy, LowDose 1–10 Gy, and HighDose >10 Gy (Figure 1B). For patients who received SRS in 3 fractions (N = 12), the linear-quadratic model with α/β for brain parenchyma = 2 Gy[9] was used to calculate corresponding dose regions: <1.31 Gy (Reference), 1.31–16.2 Gy (LowDose), and >16.2 Gy (HighDose). Changes in tissue diffusivity and vascular function were assessed in normal-appearing brain tissue in the LowDose and HighDose regions (Figure 1C). The volume of normal-appearing brain in the LowDose and HighDose regions at all follow-up MRIs are provided in Supplementary Table 2.

Quantification of Tissue Diffusivity and Vascular Function

The tissue diffusivity was assessed from ADC maps created directly on the MRI scanner from the diffusion-weighted images, using Stejskal–Tanner diffusion approximation. Vascular function was assessed by analysis of the perfusion MRI as previously described.[10] In short, standard

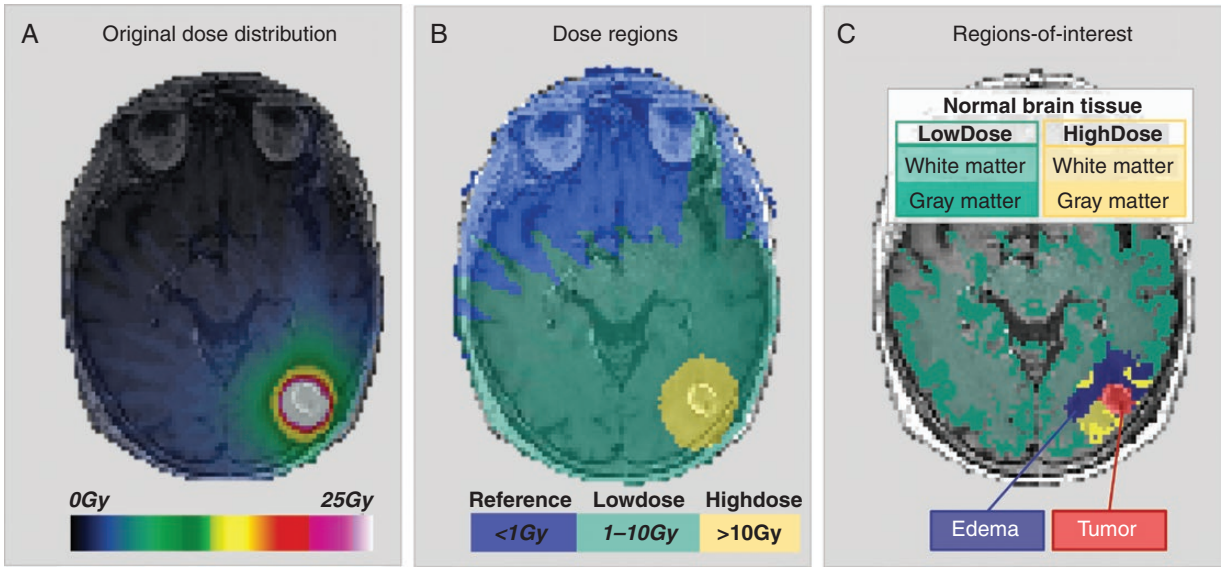

Figure 1 Regions-of-interests used for assessment of normal-appearing brain tissue responses to SRS. (A) A representative co-registered stereotactic dose distribution for a patient with brain metastasis from non-small cell lung cancer as an overlay of a T1-weighted post-contrast image acquired pre-SRS. The prescribed SRS dose was 25 Gy. (B) The dose distribution was divided into 3 dose regions: Reference: <1 Gy (blue overlay), LowDose: 1–10 Gy (green overlay), and HighDose: >10 Gy (yellow overlay). (C) The final regions-of-interest used for longitudinal response assessments included normal-appearing brain tissue, ie, white and gray matter in LowDose (white matter: light green overlay, gray matter: dark green overlay) and HighDose (white matter: light yellow overlay, gray matter: dark yellow overlay), excluding edema (purple overlay) and tumor (red overlay).

voxel-wise DSC MRI kinetic analyses of the spin- and gradient-echo acquisitions were performed in nordicICE, providing parametric maps of cerebral blood volume (CBV) and cerebral blood flow (CBF). Whereas the spin-echo maps reflect the micro-vasculature, the gradient-echo maps represent the total micro-to-macroscopic vasculature, and the prefixes "Micro" and "Macro" are henceforth used for vascular metrics obtained from spin-echo and gradient-echo, respectively. The DSC MRI analysis included motion correction, automatic detection of the arterial input function with deconvolution by standard single value decomposition, and contrast agent leakage-correction adapted for both T1- and T2-shortening effects. Vessel caliber analysis was performed in Matlab (v.R2017a, MathWorks Inc.), providing estimations of mean vessel calibers and mean vessel densities.[11]

From all MRI exams, normalized parametric maps were calculated by dividing all image voxel values to the respective median value of white matter within the Reference region (Figure 1B), henceforth prefixed *n*. For each normalized parametric map, the mean value, excluding outliers >3 SD away from the mean, of all regions-of-interests were computed if >8 non-zero voxels were present. Longitudinal changes were assessed relative to pre-SRS in percent (%), mean ± SD.

Spin-echo readout data were missing for the following number of patients: N = 2 (pre-SRS), N = 1 (+3 months), N = 2 (+6 months), N = 1 (+9 months), N = 2 (+12 months), and N = 1 (+18 months). Thus, *n*Micro-CBV and *n*Micro-CBF, as well as *n*Mean vessel calibers and *n*Mean vessel densities, could not be calculated for these patients at the given MRI exams.

ECOG Performance Status and Eloquent Regions

Pre-SRS, the Eastern Cooperative Oncology Group (ECOG) performance status was recorded for 31 of the patients as follows: 0 (N = 13), 1 (N = 16), and 2–3 (N = 2). Potential differences in normal-appearing tissue responses were assessed in patients with pre-SRS ECOG status 0 versus >0. Due to missing spin-echo data, the final number of patients assessed were (ECOG = 0/>0) N = 12/17 (pre-SRS), N = 11/15 (+3 months), N = 9/10 (+6 months), N = 7/8 (+9 months), N = 6/4 (+12 months), and N = 6/4 (+18 months).

Binary masks of all the study metastases, as well as any additional metastases also treated with SRS at the same time, were co-registered to the MNI space for assessment of their location related to eloquent regions determined from binary masks provided by the SPM12.

Statistical Analysis

Mann–Whitney U test or Fisher's exact test was used to compare groups of continuous and dichotomized data, respectively. Comparisons between absolute and relative changes (to pre-SRS) in the regions-of-interest were made using the Wilcoxon signed-rank test. The significance level was 5%, including Holm-Bonferroni correction in the case

of multiple comparisons. The statistical analyses were performed using Matlab or IBM SPSS Statistics (v25).

Results

Diffusivity and Vascular Profiles of the Pre-irradiated Brain

Compared to the LowDose and HighDose regions, the metastases and associated edema displayed pathologic diffusivity and vascular function pre-SRS (Figure 2). In the tumor, the *n*ADC ($P < .001$), *n*Macro-CBV ($P < .01$), *n*Macro-CBF ($P < .05$), and *n*Mean vessel calibers ($P < .001$) were elevated, while *n*Micro-CBF ($P < .01$) and *n*Mean vessel densities ($P < .001$) were lower. Associated edema showed higher *n*ADC ($P < .001$), *n*Micro-CBV, *n*Micro-CBF, *n*Macro-CBV, and *n*Macro-CBF ($P < .001$) and lower *n*Mean vessel densities ($P < .001$) compared to normal-appearing brain tissue (Supplementary Table 3).

In the LowDose and HighDose regions, the gray matter was characterized by higher diffusivity and increased vascular function compared to white matter, with mean gray-to-withe matter ratios of 1.2 for *n*ADC, and ranging from 1.1 to 1.8 for the vascular metrics (Supplementary Table 4).

The HighDose region of patients set to receive 3 fractions to a minimum of 1 metastasis versus a single fraction showed lower vascular metrics. Specifically, *n*Micro-CBV was 1.22 ± 0.20 versus 1.44 ± 0.21 ($P < .01$), *n*Micro-CBF was 1.23 ± 0.20 versus 1.48 ± 0.28 ($P < .05$), and *n*Mean vessel densities was 0.83 ± 0.19 versus 0.98 ± 0.12 ($P < .05$). Furthermore, the LowDose region showed lower *n*Macro-CBV in patients having received the previous radiotherapy to the brain compared with those who had not ($P < 0.05$) (Supplementary Table 5). No differences in vascular function in the LowDose and HighDose regions were observed between patients treated with or without corticosteroids (Supplementary Table 6). However, slightly higher *n*ADC was observed in the LowDose region in patients treated with corticosteroids (1.14 ± 0.05) compared to untreated patients (1.11 ± 0.05) ($P < .05$). Moreover, no differences in diffusivity or vascular function were observed between patients with different primary diagnosis (Supplementary Table 7), or between patients having received previous immunotherapy or not (Supplementary Table 8), or between patients with pre-SRS ECOG status 0 versus >0 (Supplementary Table 9). No differences in the absolute or relative change in tumor or edema volumes were observed depending on the pre-SRS ECOG status at any of the MRI examinations. However, patients with EOCG status >0 more frequently presented

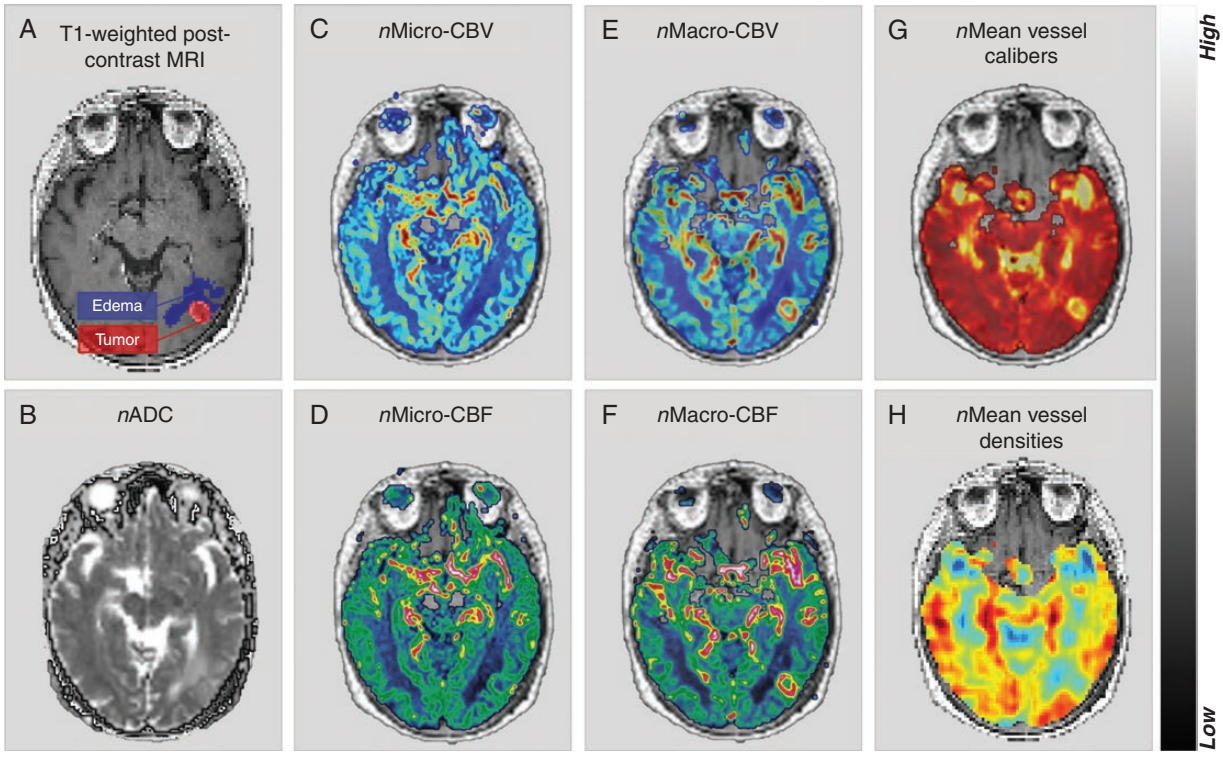

Figure 2 Normalized parametric maps of diffusivity and vascular function pre-SRS. (A) T1-weighted post-contrast image in DSC space with a brain metastasis from non-small cell lung cancer (red overlay) and associated edema (purple overlay), and normalized (*n*) parametric maps; (B) the apparent diffusion coefficient (*n*ADC), (C) *n*Micro-vascular cerebral blood volume (CBV), (D) *n*Micro-vascular cerebral blood flow (CBF), (E) *n*Macro-CBV, (F) *n*Macro-CBF, (G) *n*Mean vessel calibers, and (H) *n*Mean vessel densities.

with metastases in eloquent regions at pre-SRS ($P < .05$) (Supplementary Table 10).

Increased Diffusivity and Reduced Vascular Function of Normal Irradiated Brain

Following SRS, the LowDose region showed increased diffusivity (Figure 3Ai) combined with reduced vascular function for up until 18 months (Figure 3Bi–vi). The increase in *n*ADC in LowDose peaked 1 year post-SRS at 105.1% ± 6.1% ($P < .001$), returning to 102.5% ± 4.1% at 18 months post-SRS. Similarly, an increasing trend was observed for *n*ADC in HighDose, also peaking 1 year post-SRS at 109.6% ± 18.8%, but with larger interpatient variations.

The vascular responses in the LowDose region showed transient reduction in *n*Micro-CBV (Figure 3Bi) and *n*Micro-CBF (Figure 3Bii), combined with stable levels of *n*Macro-CBV (Figure 3Diii) and *n*Macro-CBF (Figure 3Biv), as well as transient increase in *n*Mean vessel calibers (Figure 3Bv) and reduction in *n*Mean vessel densities (Figure 3Bvi). Eighteen months post-SRS, the vascular function in the

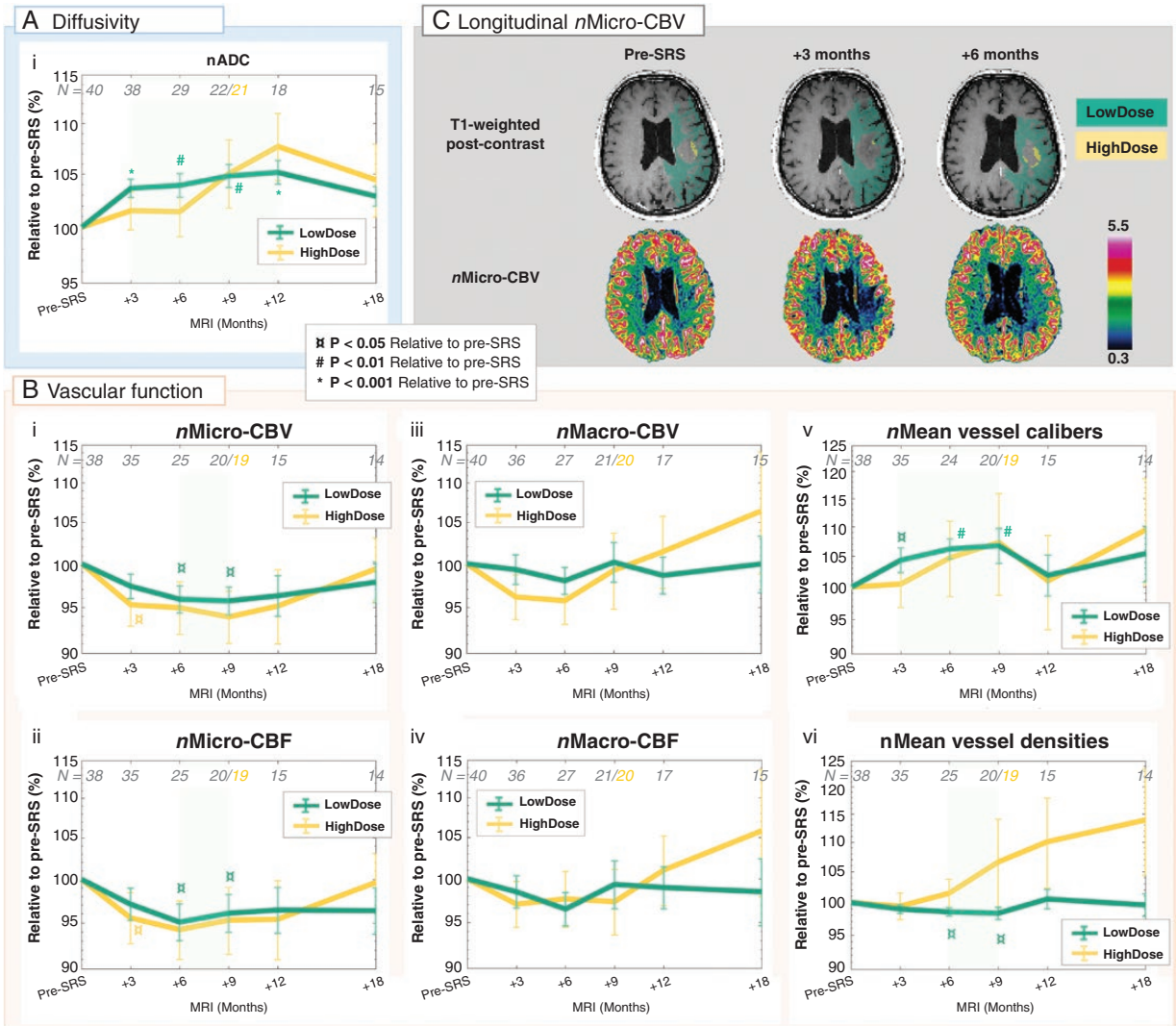

Figure 3 Increased diffusivity and decreased vascular function in normal-appearing brain up until 18 months post-SRS. Mean ± SEM of normalized (*n*) metrics relative to pre-SRS (%) in normal-appearing brain tissue in LowDose (green) and HighDose (yellow) on a logarithmic scale: (A*i*) the apparent diffusion coefficient (*n*ADC), (B*i*) *n*Micro-vascular blood volume (CBV), (B*ii*) *n*Micro-vascular blood flow (CBF), (B*iii*) *n*Macro-CBV, (B*iv*) *n*Macro-CBF, (B*v*) *n*Mean vessel calibers, and (B*vi*) *n*Mean vessel densities. Transient changes in diffusivity and vascular function are highlighted by shaded green areas. The number of patients (*N*) included at each time point is shown in gray. At 9 months post-SRS, analysis of the HighDose region was excluded for one patient due to insufficient number of voxels in this region (total number of patients analyzed is shown in yellow). (C) Reduced *n*Micro-CBV in LowDose at 3 and 6 months post-SRS compared to pre-SRS is shown for a patient with a brain metastasis from malignant melanoma (bottom row), with corresponding T1-weighted post-contrast images indicating LowDose (green) and HighDose (yellow) regions (top row). *P* values from the Wilcoxon Singed-Rank test relative to pre-SRS.

LowDose region had returned to pre-SRS levels. In the HighDose region, similar trends as in LowDose were observed for *n*Micro-CBV and *n*Micro-CBF, as well as *n*Mean vessel calibers. However, *n*Macro-CBV and *n*Macro-CBF and *n*Mean vessel densities showed a continued increasing trend from 6, 9, and 3 months post-SRS, respectively.

No apparent dose-dependency or plateau dose of the responses in diffusivity or vascularity was observed (Supplementary Figure 2). Moreover, the responses in the LowDose region for *n*Micro-CBV and *n*Micro-CBF, as well as *n*Mean vessel calibers, were different for patients with pre-SRS ECOG 0 versus >0 (Figure 4). Specifically, patients with ECOG status >0 showed transient reductions in *n*Micro-CBV to 93.6% ± 8.9% ($P < .05$) at 6 months and to 94.1% ± 4.8% at 9 months ($P < .01$; Figure 4A). The reduction at 9 months was significantly lower than for patients with pre-SRS ECOG of 0 ($P < .01$), showing a small increase of 101.6% ± 7.3%. Likewise, the transient reductions in *n*Micro-CBF at 6–9 months ($P < .01$) were lower for patients with pre-SRS ECOG >0 versus 0 at 9 months ($P < .01$) and 1 year post-SRS ($P < .05$; Figure 4B). Finally, at 6 months post-SRS, *n*Mean vessel calibers was increased to 109.6% ± 8.8% ($P < .01$) in the pre-SRS ECOG >0 patients compared to stable levels of 100.4% ± 6.2% for the patients with ECOG status 0 ($P < .05$; Figure 4C).

Discussion

In our study of 40 patients with brain metastases from non-small cell lung cancer and malignant melanoma, we show by MRI that normal-appearing brain tissue having received low doses (1–10 Gy) from SRS displays increased diffusivity and decreased vascular function for up until 18 months post-SRS. The decreased vascular function was particularly expressed by reduced levels of microvascular CBV and CBF, as well as reduced vessel densities. While no apparent changes to SRS in normal-appearing tissue were observed on conventional MRI, our findings indicate that the micro-vasculature is particularly vulnerable, even to low-dose irradiation. Combined with the observed stable levels of total CBV and CBF, as well as increases in vessel calibers, our results further imply that the vasculature of the irradiated normal brain loses radio-sensitive, yet well-functioning and highly differentiated small capillaries. Instead, the post-radiated tissue is dominated by larger vessels with potentially reduced function.

The radiation-induced effects on endothelial vascular injury in both tumors and normal tissues are known to modulate angiogenesis and neovascularization.[12] Our findings in humans are in line with preclinical studies showing that doses as low as 2 Gy may induce significant reductions of small capillaries (diameter ≤10 μm). Moreover, endothelial apoptosis caused by irradiation has been shown to induce increased vessel dilation and vessel permeability and thus reduced vascular function.[7] Interestingly, in our study we observed consistent increase in mean vessel densities from 6 months post-SRS in normal-appearing brain tissue regions having received high doses (>10 Gy) compared to low doses (1–10 Gy). Approximately 90% of endothelial cells receiving conventional fractionated radiotherapy experience mitotic cell death without apoptosis, whereas higher doses also induce apoptotic cell death.[12] Such chronic effects are commonly reflected in upregulated endothelial cell senescence in the cerebral vascular system. The observed abnormal vascular response, and especially in the HighDose region, could therefore suggest abnormal revascularization from capillary rarefaction, increased vascular permeability, and impaired vascular homeostasis.

Histopathology of patient specimens of various cerebral neoplasms with radiation-induced injury shows that damaged tissue, in addition to vascular changes, is characterized by macrophage invasion, demyelination,

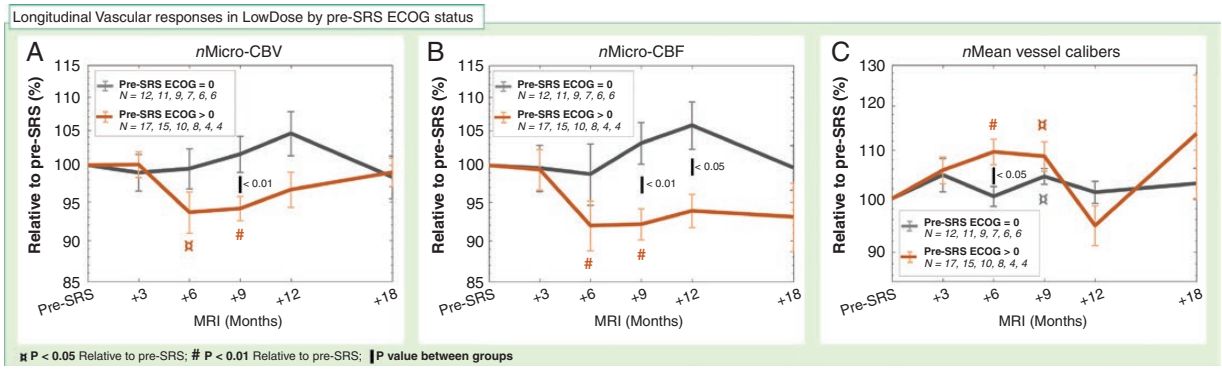

Figure 4 Reduced vascular function in normal-appearing brain is more pronounced in a patient with pre-SRS ECOG status >0 compared to 0. Mean ± SEM of normalized (*n*) metrics relative to pre-SRS (%) in normal-appearing brain tissue in LowDose on a logarithmic scale for patients with pre-SRS Eastern Cooperation Oncology Group (ECOG) status of 0 (gray) and >0 (brown). (A) Transiently reduced *n*Micro-vascular blood volume (CBV) and (B) *n*Micro-vascular blood flow (CBF) in patients with pre-SRS ECOG status >0 compared to increased *n*Micro-CBV at 9–12 months post-SRS in patients with pre-SRS ECOG status 0. (C) Transient increase in *n*Mean vessel calibers was higher in patients with pre-SRS ECOG status >0 compared to 0. The number of patients (*N*) with available data in each group is shown in the legend box. *P* values from Mann–Whitney *U* test (between groups) and the Wilcoxon Signed-Rank test (relative to pre-SRS).

and reactive gliosis.[13] In particular, the presence of demyelination and reactive gliosis both cause higher tissue diffusivity measured by diffusion-weighted MRI and diffusion tensor imaging (DTI).[14,15] The increased diffusivity of normal-appearing tissue observed in our study may be due to microstructural loss caused by such processes. Recent DTI studies have demonstrated increased diffusivity of normal-appearing white matter after fractionated radiotherapy of primary brain tumors, attributed to demyelination, and correlated with neurological deficits.[16,17] Specifically, in one of these studies including 54 adult patients, increased diffusivity in white matter beneath the cingulate cortex at 3 and 6 months after radiotherapy was associated with a decline in verbal set-shifting ability and cognitive flexibility.[17] In light of these findings, our results reinforce the potential future clinical value of using advanced MRI to identify dose tolerances to subclinical microstructural changes that can be integrated into the treatment planning and subsequently reduce neurocognitive decline.

The responses in diffusivity and vascular function of normal-appearing brain tissue in HighDose (>10 Gy), mainly representing peri-tumoral tissue, showed similar trends as in LowDose up until 1 year post-SRS. However, larger interpatient variations were observed. This may reflect variability in the pre-SRS diffusivity and vascular levels of the peri-tumoral region and consequently a different premise to handle high-dose radiation. Poor vascular function in the peri-tumoral region pre-SRS has been shown to be associated with radiation-induced changes.[10] Moreover, while at 18 months post-SRS the normal brain tissue diffusivity and vascular function in LowDose apparently returned to pre-SRS levels, all the vascular metrics showed an increasing trend starting at 6–12 months post-SRS in HighDose. The increase was particularly apparent for the *n*Macro-CBV and CBF, as well as mean vessel densities, suggesting a vascular network dominated by larger vessels and reduced capability of recruiting smaller capillaries. This deterioration of the vascular network may be a contributing factor of the underlying mechanisms involved in the development of radionecrosis—which has an increasing risk of occurring with increasing volume of brain exposed to high doses, in particular, 10 Gy and 12 Gy.[4] However, as stressed by Milano et al.[5] the development of radionecrosis is likely impacted by multiple factors, including possible regional variations in susceptibility to radiation injury. From our data, showing more homogenous tissue responses in LowDose compared to HighDose, we hypothesize that these changes also play a part in the development of radionecrosis—further supported by an occasional manifestation of radionecrosis outside the high-dose field.[6]

Although radiation exposure to normal brain tissue is reduced with SRS compared to WBRT, large volumes of normal tissue still receive low doses.[18] Our results thus support future studies on effects of low-dose irradiation for development of radionecrosis, neurologic deficits, and second malignancies.[5] Such potential long-term effects may be especially relevant with increased use of SRS to multiple and/or larger metastases, and with increasing treatment efficacy that potentially can result in longer survival times for these patients.[3]

In line with our findings, reduced CBV and CBF have been observed in normal-appearing brain tissue up until 12 months after SRS to arteriovenous malfunctions[19] and conventional radiotherapy of low- and high-grade gliomas.[20–24] In the latter studies, a dose-dependent reduction of vascular function was observed, with larger reductions in dose regions receiving more than 30% of the prescribed dose (30–66 Gy). Increased vascular responses in normal-appearing tissue during conventional radiotherapy of gliomas[8] and early after SRS to brain metastases[18] have also been reported. While a weak positive correlation between dose and increased vascular metrics, with a plateau effect at 10 Gy,[18] was observed after SRS, the strongest dose-dependency was found during the fractionated radiotherapy of the gliomas and was actually diminished 6 months post-radiotherapy. In light of our findings, showing no apparent linear correlation between responses in diffusivity or vascular function, assessed 3–18 post-SRS, the dose-dependency may be more pronounced during and early after irradiation—further indicating a dose-independent ability to restore vascular function. Altogether, the present studies having investigated advanced MRI for normal brain tissue response assessment,[17–24] including ours, demonstrate the potential for MRI metrics to identify normal brain tissue tolerances that are essential for optimizing the treatment plan accordingly.[25]

Our study observed distinctive longitudinal responses for patients having a pre-SRS ECOG status 0 compared >0. Though no apparent differences in diffusivity or vascular function were detectable by the diffusion or perfusion MRI pre-SRS, underlying subtle differences may have been present. The vasculature in normal brain tissue of patients with ECOG status >0 may already have been impaired and becoming reinforced by the radiation dose. While the association between cerebro-microvascular dysfunction and early neurologic pathogenesis is intriguing,[26,27] it is well recognized that CBF levels and cognitive impairment are inversely correlated.[28] In our study, changes in ECOG performance status could not be correlated to responses in diffusivity or vascular function as the ECOG status was not routinely recorded at the clinical follow-ups post-SRS. This is however warranted in future studies.

Our study has limitations. Outside of the study period, individual treatment management resulted in large variations with respect to previous and salvage radiation therapy to the brain, prescription dose and fractionations of the study SRS, use of immunotherapy, systemic treatment, and corticosteroid treatment. Combined with the longitudinal reduction of patients, multivariate analyses were thus not feasible. However, a separate analysis of the different treatment groups showed that excluding patients previously treated with brain radiotherapy did not alter the outcome of the longitudinal response analysis. In our study and within the power of our sample size, the patients treated with 3 fractions versus the patients treated with a single fraction did not show any apparent differences in the longitudinal changes in diffusivity or vascular function. We aimed to reduce the potential impact of different fractionation regimes on our findings by calculating equivalent doses (EQD2) for the

dose distributions delivered in 3 fractions. The validity of the linear-quadratic model is less established for higher doses (>8–10 Gy), but the LowDose region is mainly dominated by doses <10 Gy and should therefore be less influenced by this restriction. The lower pre-SRS perfusion levels in what later became the HighDose region in patients receiving 3 rather than a single SRS fraction may well be due to differences in tumor size. Larger tumors, more commonly treated with fractionated SRS, may inherently be more prone to reduced vascular function in the peri-tumoral region.[10] Thus, although receiving less than 10 Gy per fraction, which has been shown to be a threshold dose for inducing apoptotic endothelial cells death,[12] the impaired pre-SRS vasculature may reduce the level of this threshold dose. Furthermore, no differences in pre-SRS diffusivity and vascular function of normal brain tissue or longitudinal responses were present between patients having received immunotherapy or not. However, preliminary analysis of the current study population does imply that concomitant SRS and immunotherapy render peri-tumoral regions more prone to changes than SRS alone,[29] indicating dose-dependent synergetic effect immunotherapy to SRS. Finally, corticosteroid treatment has been suggested to decrease vascular functions, but conflicting results are reported in the literature.[30,31] Due to lack of information about corticosteroid use on the follow-up MRIs, this could not be account for in our data. However, at pre-SRS no differences in any vascular metrics were observed between patients using corticosteroids and not.

Our longitudinal MRI study indicates that normal brain tissue is sensitive to low doses of irradiation following SRS, resulting in loss of, and potentially, reduced ability to form well-functioning capillaries. The long-term implications of our findings in terms of neurological function and clinical outcomes are thus warranted in future studies.

Supplementary Data

Supplementary data are available at *Neuro-Oncology Advances* online.

Keywords

brain metastases | diffusion-weighted MRI | normal-appearing brain tissue response | perfusion MRI | stereotactic radiosurgery

Funding

This work was supported by the South-Eastern Norway Regional Health Authority (2016102, 2013069); the Norwegian Cancer Society (6817564); the European Research Council under the European Union's Horizon 2020 (758657); and the Research Council of Norway (261984).

Acknowledgments

We thank Dr. Knut Håkon Hole at Oslo University Hospital for a constructive review of the manuscript.

Conflict of interest statement. Intellectual property right, NordicNeuroLab AS, Bergen, Norway (K.E.E).

Authorship Statement. Experimental design: L.B.N, C.S., K.D.J., Å.H., and K.E.E. Implementation: L.B.N, I.D, E.G., C.S., O.G., K.D.J., Å.H., and K.E.E. Analysis and/or interpretation of the data: L.B.N., I.D., E.G., C.S., A.L., D.O.S., and K.E.E. Writing of the first manuscript draft: L.B.N., I.D., E.G., C.S., A.L., D.O.S., and K.E.E. Editing: all coauthors. Read and approved the final version: all coauthors. Unpublished material: no unpublished material is referenced.

References

1. Hartgerink D, van der Heijden B, De Ruysscher D, et al. Stereotactic radiosurgery in the management of patients with brain metastases of non-small cell lung cancer: indications, decision tools and future directions. *Front Oncol.* 2018;8(9):154.
2. Chang EL, Wefel JS, Hess KR, et al. Neurocognition in patients with brain metastases treated with radiosurgery or radiosurgery plus whole-brain irradiation: a randomised controlled trial. *Lancet Oncol.* 2009;10(11):1037–1044.
3. Schimmel WCM, Gehring K, Eekers DBP, Hanssens PEJ, Sitskoorn MM. Cognitive effects of stereotactic radiosurgery in adult patients with brain metastases: a systematic review. *Adv Radiat Oncol.* 2018;3(4):568–581.
4. Minniti G, Clarke E, Lanzetta G, et al. Stereotactic radiosurgery for brain metastases: analysis of outcome and risk of brain radionecrosis. *Radiat Oncol.* 2011;6(15):48.
5. Milano MT, Usuki KY, Walter KA, Clark D, Schell MC. Stereotactic radiosurgery and hypofractionated stereotactic radiotherapy: normal tissue dose constraints of the central nervous system. *Cancer Treat Rev.* 2011;37(7):567–578.
6. Sundgren PC, Cao Y. Brain irradiation: effects on normal brain parenchyma and radiation injury. *Neuroimaging Clin N Am.* 2009;19(4):657–668.
7. Belka C, Budach W, Kortmann RD, Bamberg M. Radiation induced CNS toxicity—molecular and cellular mechanisms. *Br J Cancer.* 2001;85(9):1233–1239.
8. Cao Y, Tsien CI, Sundgren PC, et al. Dynamic contrast-enhanced magnetic resonance imaging as a biomarker for prediction of radiation-induced neurocognitive dysfunction. *Clin Cancer Res.* 2009;15(5):1747–1754.
9. Brenner DJ. The linear-quadratic model is an appropriate methodology for determining isoeffective doses at large doses per fraction. *Semin Radiat Oncol.* 2008;18(4):234–239.
10. Digernes I, Grøvik E, Nilsen LB, et al. Brain metastases with poor vascular function are susceptible to pseudoprogression after stereotactic radiation surgery. *Adv Radiat Oncol.* 2018;3(4):559–567.

11. Emblem KE, Farrar CT, Gerstner ER, et al. Vessel caliber—a potential MRI biomarker of tumour response in clinical trials. *Nat Rev Clin Oncol.* 2014;11(10):566–584.
12. Venkatesulu BP, Mahadevan LS, Aliru ML, et al. Radiation-induced endothelial vascular injury: a review of possible mechanisms. *JACC Basic Transl Sci.* 2018;3(4):563–572.
13. Sundgren PC, Fan X, Weybright P, et al. Differentiation of recurrent brain tumor versus radiation injury using diffusion tensor imaging in patients with new contrast-enhancing lesions. *Magn Reson Imaging.* 2006;24(9):1131–1142.
14. Hagen T, Ahlhelm F, Reiche W. Apparent diffusion coefficient in vasogenic edema and reactive astrogliosis. *Neuroradiology.* 2007;49(11):921–926.
15. Natarajan R, Hagman S, Wu X, et al. Diffusion tensor imaging in NAWM and NADGM in MS and CIS: association with candidate biomarkers in Sera. *Mult Scler Int.* 2013;2013:265259.
16. Chapman CH, Nagesh V, Sundgren PC, et al. Diffusion tensor imaging of normal-appearing white matter as biomarker for radiation-induced late delayed cognitive decline. *Int J Radiat Oncol Biol Phys.* 2012;82(5):2033–2040.
17. Tringale KR, Nguyen T, Bahrami N, et al. Identifying early diffusion imaging biomarkers of regional white matter injury as indicators of executive function decline following brain radiotherapy: a prospective clinical trial in primary brain tumor patients. *Radiother Oncol.* 2019;132(March):27–33.
18. Jakubovic R, Sahgal A, Ruschin M, Pejović-Milić A, Milwid R, Aviv RI. Non tumor perfusion changes following stereotactic radiosurgery to brain metastases. *Technol Cancer Res Treat.* 2015;14(4):497–503.
19. Taki S, Higashi K, Oguchi M, et al. Changes in regional cerebral blood flow in irradiated regions and normal brain after stereotactic radiosurgery. *Ann Nucl Med.* 2002;16(4):273–277.
20. Fahlström M, Blomquist E, Nyholm T, Larsson EM. Perfusion magnetic resonance imaging changes in normal appearing brain tissue after radiotherapy in glioblastoma patients may confound longitudinal evaluation of treatment response. *Radiol Oncol.* 2018;52(2):143–151.
21. Fuss M, Wenz F, Scholdei R, et al. Radiation-induced regional cerebral blood volume (rCBV) changes in normal brain and low-grade astrocytomas: quantification and time and dose-dependent occurrence. *Int J Radiat Oncol Biol Phys.* 2000;48(1):53–58.
22. Lee MC, Cha S, Chang SM, Nelson SJ. Dynamic susceptibility contrast perfusion imaging of radiation effects in normal-appearing brain tissue: changes in the first-pass and recirculation phases. *J Magn Reson Imaging.* 2005;21(6):683–693.
23. Petr J, Platzek I, Seidlitz A, et al. Early and late effects of radiochemotherapy on cerebral blood flow in glioblastoma patients measured with non-invasive perfusion MRI. *Radiother Oncol.* 2016;118(1):24–28.
24. Price SJ, Jena R, Green HA, et al. Early radiotherapy dose response and lack of hypersensitivity effect in normal brain tissue: a sequential dynamic susceptibility imaging study of cerebral perfusion. *Clin Oncol (R Coll Radiol).* 2007;19(8):577–587.
25. Balagamwala EH, Chao ST, Suh JH. Principles of radiobiology of stereotactic radiosurgery and clinical applications in the central nervous system. *Technol Cancer Res Treat.* 2012;11(1):3–13.
26. Toth P, Tarantini S, Csiszar A, Ungvari Z. Functional vascular contributions to cognitive impairment and dementia: mechanisms and consequences of cerebral autoregulatory dysfunction, endothelial impairment, and neurovascular uncoupling in aging. *Am J Physiol Heart Circ Physiol.* 2017;312(1):H1–H20.
27. Østergaard L, Aamand R, Gutiérrez-Jiménez E, et al. The capillary dysfunction hypothesis of Alzheimer's disease. *Neurobiol Aging.* 2013;34(4):1018–1031.
28. Alosco ML, Gunstad J, Jerskey BA, et al. The adverse effects of reduced cerebral perfusion on cognition and brain structure in older adults with cardiovascular disease. *Brain Behav.* 2013;3(6):626–636.
29. Nilsen LB, Groevik E, Digernes I, et al. Vascular responses in normal brain tissue after combined immunotherapy and SRS to brain metastases. Radiother Oncol. 2019;133(Suppl 1):S551–S552.
30. Bastin ME, Carpenter TK, Armitage PA, Sinha S, Wardlaw JM, Whittle IR. Effects of dexamethasone on cerebral perfusion and water diffusion in patients with high-grade glioma. *AJNR Am J Neuroradiol.* 2006;27(2):402–408.
31. Koedel U, Pfister HW, Tomasz A. Methylprednisolone attenuates inflammation, increase of brain water content and intracranial pressure, but does not influence cerebral blood flow changes in experimental pneumococcal meningitis. *Brain Res.* 1994;644(1):25–31.